

Excited States in  $B^{11}$  Observed in the  $Li^7(\alpha\gamma)$  Reaction\*

P. PAUL† AND N. G. PUTTASWAMY‡

*Department of Physics, Stanford University, Stanford, California*

AND

D. KOHLER§

*Department of Physics, Stanford University, Stanford, California and  
Lockheed Palo Alto Research Laboratory, Palo Alto, California*

(Received 4 August 1967)

Excited states in  $B^{11}$  between 9.5 and 11 MeV were studied by use of the  $Li^7(\alpha,\gamma)B^{11}$  and  $Li^7(\alpha,\alpha')Li^{7*}$  (478 keV) reactions. The thin-target excitation function of the capture reaction, which was obtained at  $90^\circ$  for the ground-state transition from 1.3- to 3.2-MeV bombarding energy, displays a structured peak around 2.5 MeV with a peak differential cross section of  $2 \mu\text{b}/\text{sr}$ . A transition to the first excited state was not observed, setting an upper limit for  $d\sigma/d\Omega < 0.2 \mu\text{b}/\text{sr}$ . By comparing the yield with that of the  $C^{13}(p,\gamma_0)N^{14}$  reaction, an absolute peak cross section of  $22.5 \mu\text{b}/\text{sr}$  ( $\pm 20\%$ ) was obtained for the 951-keV resonance. Reinvestigation of the inelastic scattering cross section over the same bombarding energy range, coupled with a Breit-Wigner analysis, yielded for the states at 9.87, 10.26, and 10.62 MeV the assignments for spin and parity of  $\frac{3}{2}^+$ ,  $\frac{1}{2}^\pm$  or  $\frac{3}{2}^\pm$ , and  $\frac{5}{2}^+$ , respectively. This is essentially in agreement with the recent work by Cusson on elastic and inelastic  $\alpha$  scattering. Analysis of the radiative capture cross sections (assuming isotropy) with resonance parameters from the particle reactions gives the following ground-state  $\gamma$  widths for the established states:  $< 0.5$  eV (at 9.88 MeV); 17 eV (10.26 MeV); 1 eV (10.32 MeV);  $\leq 0.2$  eV (10.61 MeV). There is evidence for a new state at  $10.45 \pm 0.05$  MeV with  $\Gamma(\text{c.m.}) \sim 140$  keV and  $(2J+1)\Gamma_\gamma = 10$  eV. Possible analog states in  $C^{11}$  have been reinvestigated with the  $B^{10}(p,\gamma_0)C^{11}$  reaction. The  $\gamma$  transition strengths observed in  $B^{11}$  do not agree with present shell-model calculations.

## 1. INTRODUCTION

THE electromagnetic decay properties of nuclear states in  $B^{11}$  have been studied extensively up into the region of the lowest unbound levels, including that at 9.28 MeV. A comprehensive discussion of experimental and theoretical knowledge pertinent to all states below 9 MeV can be found in the recent publication by Olness *et al.*<sup>1</sup> In general, agreement between the level energy as well as  $M1$  transition strengths of odd parity states and the intermediate coupling calculation by Cohen and Kurath<sup>2</sup> is fairly good. With the exception of the  $\frac{3}{2}^-$  state at 8.57 MeV,<sup>1</sup> all normal parity states required by the shell model, and only these, are found experimentally in this region. Above the 9.28-MeV, state, a number of broad states are known to exist.<sup>3</sup> The spin-parity assignments of these states are not securely established, nor have radiative-decay properties been investigated. The intermediate coupling model predicts eight additional odd parity states between 9 MeV and the first  $T = \frac{3}{2}$  state, i.e., about 13 MeV, three of which are expected below 12 MeV. The work presented here was directed at finding levels

and/or establishing some radiative decay properties up to an excitation energy of 10.7 MeV through study of the capture reaction  $Li^7(\alpha,\gamma)B^{11}$ . Since states in this region are expected to have an increasingly large width, the capture reaction offers in many cases the only feasible way of studying electromagnetic transitions from such states. The same reaction has been explored by several authors<sup>4,5</sup> at the narrow resonances at 401-, 815-, and 951-keV bombarding energy associated with states at 8.92, 9.19, and 9.28 MeV, respectively. At higher bombarding energies the inelastic-scattering channel to the 478-keV state in  $Li^7$  becomes available. This fact and the increasing strength of the elastic channel, in general, tend to decrease the radiative capture cross section into the  $\mu\text{b}$  regime. With a detection system especially designed for small cross-section measurements, we extended the study of the capture reaction up to a bombarding energy of 3 MeV. Interfering background reactions limited the experiment to observation of the transitions to ground and first excited states.

Reliable information about the existence of levels in this region comes mainly from the reactions  $B^{10}(d,p)B^{11}$  and  $Li^7(\alpha,\alpha')$ . In the stripping reaction Groce *et al.*<sup>6</sup> found levels at excitation energies of 9.87, 10.34, 10.59, and possibly at 10.26 MeV. Presumably all these levels have widths of less than about 400 keV in order to be observed in the proton spectrum. Inelastic  $\alpha$  scattering

\* Research supported by the National Science Foundation.

† A. P. Sloan Foundation Fellow. Present address: Department of Physics, State University of New York, Stony Brook, New York.

‡ Present address: Physics Division, Argonne National Laboratory, Argonne, Illinois.

§ Present address: Lockheed Palo Alto Research Laboratory, Palo Alto, California.

<sup>1</sup> J. W. Olness, E. K. Warburton, D. E. Alburger, and J. A. Becker, *Phys. Rev.* **139**, B512 (1965).<sup>2</sup> S. Cohen and D. Kurath, *Nucl. Phys.* **73**, 1 (1965).<sup>3</sup> F. Ajzenberg-Selove and T. Lauritsen, *Nucl. Phys.* **11**, 1 (1959).<sup>4</sup> G. A. Jones, C. M. P. Johnson, and D. H. Wilkinson, *Phil. Mag.* **4**, 796 (1959).<sup>5</sup> L. L. Green, G. A. Stephens, and J. C. Willmott, *Proc. Phys. Soc. (London)* **79**, 1017 (1962).<sup>6</sup> D. E. Groce, J. H. McNally, and W. Whaling, *Bull. Am. Phys. Soc.* **8**, 486 (1963).

has been studied by several authors,<sup>7,8</sup> and most recently by Cusson.<sup>9</sup> All groups report peaks in the excitation function at 9.88-, 10.26-, and 10.62-MeV excitation energy. Cusson<sup>9</sup> also presents data on elastic scattering. Combining the elastic and inelastic (478 keV) cross sections, henceforth called  $E$  and  $I$ , respectively, the two-channel problem can be solved for a set of partial widths. With the help of these, one can extract the radiative width from the capture cross section at any resonance which is observed in the capture reaction. Alternatively, making use of  $R$ -matrix theory explicitly for the energy dependence of  $I$  and the capture reaction, henceforth called  $C$ , the radiative widths may be obtained from  $I$  and  $C$  alone with reasonable assumptions about interaction radii and reduced widths. Since the analysis of  $E$  by Cusson<sup>9</sup> turned out to be less than straightforward, we will present the results of both analyzing procedures. The results obtained for several levels near 10 MeV will be compared with the predictions of the shell model and with the available information on the known levels in the corresponding energy region of C<sup>11</sup>.

## 2. EXPERIMENTAL PROCEDURE

The experiment measured the cross sections for inelastic  $\alpha$  scattering and radiative  $\alpha$  capture by Li<sup>7</sup> for bombarding energies between 1 and 3.2 MeV. The magnetically analyzed He<sup>4</sup> beam of the Stanford 3-MV Van de Graaff accelerator entered a glass target chamber through an in-line cold trap. Targets were prepared by evaporating isotopically enriched (99.97%) metallic Li<sup>7</sup> inside the target chamber onto a thick copper backing. Various target thicknesses between 10 and 70 keV (for 1-MeV  $\alpha$  particles) were used.

### A. $\gamma$ -Detection System

The main difficulty in measuring the capture reaction ( $C$ ) cross section arises from the inherently small value ( $\sim 10 \mu\text{b}$ ). A  $\gamma$ -detection system designed specifically for the measurement of such small cross sections in the presence of a large background at lower energies has been described previously.<sup>10</sup> The arrangement used for this experiment is indicated schematically in Fig. 1. Compared to the older system it incorporates improvements in both geometry and electronics. These are described in detail elsewhere.<sup>11</sup> Briefly, the main features are as follows:

A 5-in.  $\times$  6-in. cylindrical NaI(Tl) crystal is surrounded by a plastic (NE 102) anticoincidence shield, approximately 5 in. thick (see Fig. 1). This shield sur-

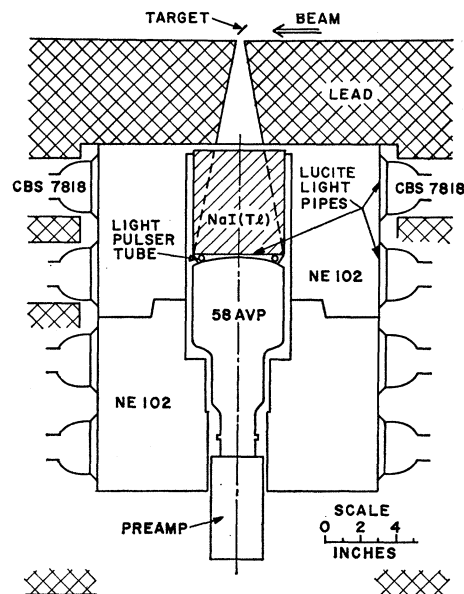


FIG. 1. The  $\gamma$ -detection system showing the NaI center crystal and NE102 anticoincidence plastic shield.

rounds the NaI crystal very closely and extends far back past the photomultiplier. It therefore not only greatly reduces cosmic-ray background, but, more importantly, improves the  $\gamma$  ray response function by rejecting from analysis a large portion of those events in which energy has escaped from the center crystal. The total assembly was shielded by approximately 8 in. of lead on all sides and 10 in. on top.

The center crystal was mounted on a fast 58-AVP photomultiplier tube. Fast proportional pulses, clipped to a width of about 3 nsec, were sent to a tunnel-diode discriminator to reduce pileup in the fashion described in Ref. 11. For good response improvement in the NaI-crystal spectrum, the anticoincidence threshold in the plastic shield could be set as low as 80 keV. Cosmic-ray rejection of the system was better than 200 to 1 for  $\gamma$  energies between 10 and 20 MeV.

The present experiment involves rather large count rates in the lower part of the  $\gamma$  spectrum, i.e., below 9 MeV. Without precaution, the ensuing large photomultiplier currents make the gain very sensitive to the stability of the bombarding beam current. (This difficulty is enhanced by the choice of a fast photomultiplier.) In the present system these effects are reduced by two complementary techniques. Voltage redistribution effects along the dynode chain were diminished by applying a fixed voltage to the dynode chain at the stage supplying the proportional signal. This uncouples the later, more heavily loaded stages from the proportional part of the chain. Secondly, an electronic gain stabilization of the type described by Marlow<sup>12</sup> was incorporated. This circuit employs a small light source which generates

<sup>7</sup> H. Bichsel and T. W. Bonner, Phys. Rev. **108**, 1025 (1957); N. P. Heydenburg and G. M. Temmer, *ibid.* **94**, 1252 (1954).

<sup>8</sup> C. W. Li and R. Sherr, Phys. Rev. **96**, 1252 (1954).

<sup>9</sup> R. Y. Cusson, Nucl. Phys. **86**, 481 (1966).

<sup>10</sup> P. Paul, S. L. Blatt, and D. Kohler, Phys. Rev. **137**, B493 (1965).

<sup>11</sup> S. L. Blatt, thesis, Stanford University, 1965 (unpublished).

<sup>12</sup> K. W. Marlow, Nucl. Instr. Methods **15**, 188 (1962).

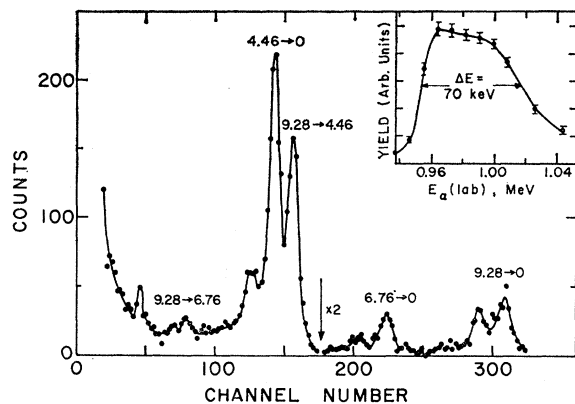


FIG. 2. Gamma spectrum obtained at  $90^\circ$  in the  $\text{Li}^7(\alpha, \gamma)\text{B}^{11}$  reaction at  $E_\alpha = 951$  keV. Various transitions from the 9.28-MeV level are indicated. The insert shows a typical yield curve taken over the narrow ( $\approx 7$  keV) 951-keV resonance.

a reference pulse and was mounted in a light pipe between the NaI crystal and photomultiplier. Its amplitude was adjusted so as to exceed the acceptance range of the analyzer and thus did not introduce additional analyzer dead time. Both improvements together produced a gain stability of better than 2% even in the presence of large beam fluctuations.

### B. Radiative Capture Transitions

The detector system was placed at  $90^\circ$  to the beam direction and the observed  $\gamma$  ray spectrum stored in a 400-channel analyzer. The geometry and collimation can be seen in Fig. 1. Figure 2 shows a  $\gamma$  spectrum obtained in the  $\text{Li}^7(\alpha, \gamma)\text{B}^{11}$  reaction at the well-known resonance at 951-keV  $\alpha$  energy. The antileup discriminator level was reduced in order to observe the transitions of lower energy. This resonance has been studied in detail by Jones *et al.*,<sup>4</sup> and Green *et al.*<sup>5</sup> The main features of Fig. 2 are in agreement with their work. Manifest are the strong transitions to the state at 4.46 MeV (67%) and the subsequent ground-state transition as well as the transition to the 6.75-MeV state (13%) with its further decays. The transition directly to ground state (20%) is clearly resolved.

The observation of capture reactions usually has to contend with relatively much more intense  $\gamma$  rays following particle reactions such as  $(\alpha, p)$  or  $(\alpha, n)$  with substantially larger cross sections. In the present case this problem is alleviated by the fact that  $(\alpha, p)$  or  $(\alpha, n)$  reactions on  $\text{Li}^7$  are endothermic by about 3.0 MeV. However, despite this advantage, at bombarding energies above 2 MeV it turned out to be impossible to investigate transitions of energy less than 7 MeV with any confidence for the following reason: Neutrons are produced by  $\alpha$  bombardment of target contaminants such as carbon or oxygen with cross sections of around 100 mb. Capture of neutrons in the  $\text{Na}^{23}$  and  $\text{I}^{127}$  of the detection crystal have  $Q$  values of 6.96 and 6.7 MeV, respectively. For most recorded events the entire decay

cascade will be absorbed in the crystal leading to prominent peaks corresponding to the  $Q$ -value energies. In evidence for the presence of neutrons a large peak at 2.26 MeV was observed due to neutron absorption into the hydrogen of the anticoincidence plastic shield. Despite use of a cold trap and a vac-ion pump on the target chamber, it proved impossible to reduce buildup of carbon and oxygen sufficiently to eliminate neutron-capture  $\gamma$  rays. This is due to the great affinity of metallic Li targets for carbon and oxygen and the fact that the targets used had to be extremely thin, typically only 4 keV thick to 1-MeV protons. Above the "neutron edge" lie the transitions to the ground and first excited states. A spectrum typical of this energy region is shown in Fig. 3. This was taken with the antileup discriminator set just below 7 MeV. While the ground-state transition was always clearly resolved in the entire range of bombarding energies, only an upper limit can be given for the transition to the first excited state. The latter value is estimated to be less than 10% of the transition to the ground state (see Fig. 3). This number is representative for the entire range of bombarding energies from 1 to 3 MeV.

### C. Calibration of the Radiative Capture Cross Section

Gamma rays which are detected in the central NaI crystal but lose energy into the anticoincidence shield are rejected before analysis. The rejection ratio is a function of  $\gamma$  energy. To obtain an absolute capture cross section from the observed number of events, the efficiency of the system has to be determined experimentally.

This was done in two ways: The first made use of the narrow resonance at 951 keV in the  $\text{Li}^7(\alpha, \gamma)\text{B}^{11}$  reaction itself. Its total width  $\Gamma$  (c.m.) has an averaged experi-

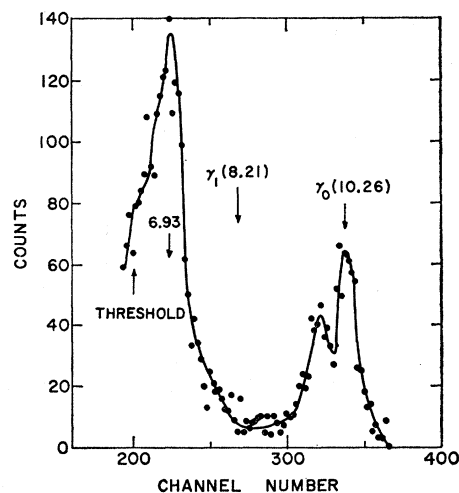


FIG. 3. High-energy  $\gamma$  spectrum obtained in the  $\text{Li}^7(\alpha, \gamma)\text{B}^{11}$  reaction at 2.50 MeV. The antileup discriminator is set at about 6 MeV. Positions of transitions to the ground and first excited states are indicated.

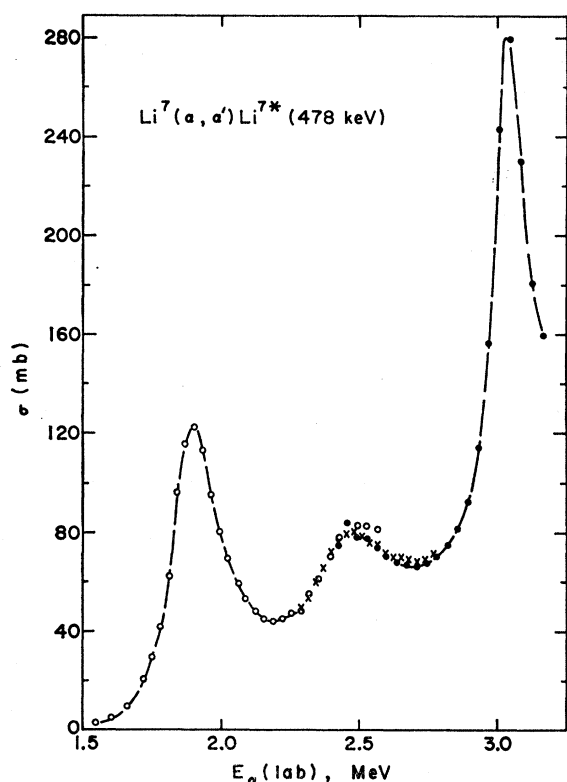


FIG. 4. Excitation function of the  $\text{Li}^7(\alpha, \alpha')\text{Li}^{7*}(478 \text{ keV})$  reaction. The total cross section is normalized to the value of Li and Sherr (Ref. 8) at 2.50 MeV.

mental value<sup>4,13</sup> of 4.1 keV. An excitation function taken over this resonance gave a target profile such as shown by the insert in Fig. 2. In this case the target thickness was 67 keV for 951-keV  $\alpha$  particles. This target profile was used to obtain the "thick target" yield for the ground-state transition. The capture cross section off resonance (assumed to be constant over the target thickness) is related to the one at resonance by<sup>10</sup>

$$\frac{d\sigma}{d\Omega} = \frac{d\sigma(\text{res})}{d\Omega} \left( \frac{\Gamma}{\xi} \frac{Y}{Y_{\text{res}}} \arctan\left(\frac{\xi}{\Gamma}\right) \right), \quad (1)$$

where  $Y_{\text{res}}$  and  $Y$  are the  $\gamma$  yields on and off resonance, respectively, and  $\xi$  is the target thickness. Since the  $\gamma$  ray energy changes only very little from  $E_{\alpha}=1$  to 3 MeV, we neglect the energy dependence of the rejection ratio. The peak cross section at the 951-keV resonance can be obtained from the work of Jones *et al.*<sup>4</sup> The branching ratios<sup>4,5</sup> and angular distribution<sup>5,14</sup> for the ground-state transition lead to a peak cross section at  $90^{\circ}$  given by  $d\sigma/d\Omega = 20 \mu\text{b/sr}$  ( $\pm 25\%$ ). With this value and Eq. (1) we obtained a cross section  $d\sigma/d\Omega = 2.0 \mu\text{b/sr}$  at  $E_{\alpha}=2.56$  MeV. The results obtained with several targets agreed to within 15%.

<sup>13</sup> S. S. Hanna and L. Meyer-Schützmeister (private communication).

<sup>14</sup> L. Meyer-Schützmeister and S. S. Hanna, *Bull. Am. Phys. Soc.* **2**, 28 (1957).

The capture cross section in the 951-keV resonance has some significance for certain astrophysical considerations. The analog reaction  $\text{Be}^7(\alpha, \gamma)\text{C}^{11}$  provides a possible path toward formation of heavier elements bypassing the unstable  $\text{Be}^8$  nucleus. The state in  $\text{C}^{11}$  which corresponds to the 951-keV resonance in  $\text{B}^{11}$  may be close enough to threshold to allow formation under certain astrophysical conditions. Until the cross section for  $\text{Be}^7(\alpha, \gamma)$  is measured directly, one can only infer a value from the analog reaction  $\text{Li}^7(\alpha, \gamma)$ . We therefore made an independent measurement of the 951-keV resonance cross section which, of course, also checks the calibration for the  $\alpha$  capture excitation function. This was done by comparing the thick target yield of the strong ground-state transition from the 9.17-MeV level in  $\text{N}^{14}$  observed in  $\text{C}^{13}(p, \gamma)$  at  $E_p=1.74$  MeV with the  $\text{Li}^7(\alpha, \gamma)$  thick target yield for the 9.28-MeV transition at the 951-keV resonance. The rejection ratio was again assumed constant over the range of  $\gamma$  energies. The cross section in  $\text{N}^{14}$  is reported as<sup>15</sup>  $(200 \pm 40)$  mb. With this value and the quoted angular distribution<sup>16</sup> this measurement yielded  $22.5 \mu\text{b/sr}$  ( $\pm 25\%$ ) for the 9.28-MeV transition on resonance at  $90^{\circ}$ , in good agreement with the value used for the first method.

#### D. Inelastic Alpha Scattering

The inelastic scattering cross section ( $I$ ) was obtained by detecting, in the NaI crystal, the 478-keV  $\gamma$  ray from the de-excitation of the first excited state of  $\text{Li}^7$ . Since this state has  $J=\frac{1}{2}$  the excitation function at any angle is proportional to the total cross section. The cross section was previously reported<sup>7</sup> to be of the order of 100 mb and this experiment posed no problems.

### 3. EXPERIMENTAL RESULTS

The excitation function obtained in the present experiment for the inelastic-scattering cross section ( $I$ ) is given in Fig. 4. Statistical errors are negligible. The total-cross-section scale was normalized to the data of Li and Sherr<sup>8</sup> by equating the yield at 2.5 MeV to 80 mb. They estimate the cross-section error to be  $\pm 20\%$ . On a relative scale, our curve agrees well with Li and Sherr<sup>7</sup> but is somewhat in disagreement with the curve of Cusson<sup>9</sup> in the region around 1.9 MeV. This will be discussed later in connection with the analysis. All authors,<sup>7-9</sup> however, agree on the essential structure observed in Fig. 4. Strong resonances occur at  $1.90 \pm 0.01$  MeV and at  $3.04 \pm 0.01$  MeV (after correcting for target thickness) and a broad maximum at 2.48 MeV.

The new contribution of this paper is the data shown in Fig. 5. The radiative capture cross section ( $C$ ) for the ground-state transitions displays remarkable struc-

<sup>15</sup> S. S. Hanna and L. Meyer-Schützmeister, *Phys. Rev.* **115**, 986 (1959).

<sup>16</sup> H. H. Woodbury, R. B. Day, and A. V. Tollestrup, *Phys. Rev.* **92**, 1199 (1953).

TABLE I. Resonances and parameters obtained from Cusson's analysis<sup>a</sup> of inelastic and elastic scattering for  $R=6.0$  F.  $d\sigma/d\Omega$  and  $\Gamma, \gamma$  are capture cross section and radiative widths relating to each state as obtained from the present data. The single-particle Wigner limit is  $\gamma_W^2=0.68$  MeV.

$E_R$ (lab) (MeV)	$E_{ex}$ in $B^{11}$ (MeV)	$J^\pi$	$\Gamma$ (c.m.) (keV)	$\gamma_{\alpha,l^2}$ (MeV)	$\gamma_{\alpha,l+z^2}$	$\gamma_{\alpha',l^2}$ (MeV)	$\Gamma_I/\Gamma_E$	$d\sigma/d\Omega$ ( $\mu\text{b}/\text{sr}$ )	$\Gamma\gamma_0$ (eV)
1.88	9.86	$\frac{3}{2}^+$	250	0.05		1.26	4.0	<0.1	<1.9
2.50	10.26	$\frac{3}{2}^-$	200	0.05	0.07	0.03	0.04	1.2	5
2.60	10.32	$\frac{3}{2}^-$	100	0.09	0.17	0.0	0.0	0.7	0.9
2.69	10.38	$\frac{3}{2}^+$	4000	0.32		2.95	4.6	0.5	310
2.75 <sup>b</sup>	10.42 <sup>b</sup>		$\sim 200$					$\sim 0.8$	
3.03	10.59	$\frac{7}{2}^+$	90	0.084		0.275	1.0	$\leq 0.12$	$\leq 0.2$

<sup>a</sup> Reference 9.

<sup>b</sup> This state is inferred from the radiative capture cross section.

ture. While there is no evidence of the 1.9-MeV resonance observed in  $I$ , the  $C$  cross section reaches a wide peak at  $2.50 \pm 0.02$  MeV with an additional peak at  $2.62 \pm 0.02$  MeV (after target thickness correction). This structure was retraced with several thinner targets in order to obtain the true resonance width. Several points from these runs are included in Fig. 5. The error on each point is quite large and contains about equal contributions from statistics and errors in spectrum analysis. The line drawn through the data points represents an estimate of the best fit. Consistently, although not outside the errors, a weak indication of the state at 3.04 MeV appears in  $C$ . The cross-section scale in Fig. 5 was established in the way discussed in Sec. 2C. As previously stated, a possible transition to the first excited state at 2.14 MeV amounts, in the entire range, to less than 10% of the ground-state transition.

#### 4. ANALYSIS

Analysis is based on the  $R$ -matrix theory specialized to the case of two open channels, i.e., the elastic and inelastic [ $Li^{7*}(478 \text{ keV})$ ]  $\alpha$ -scattering channels. The

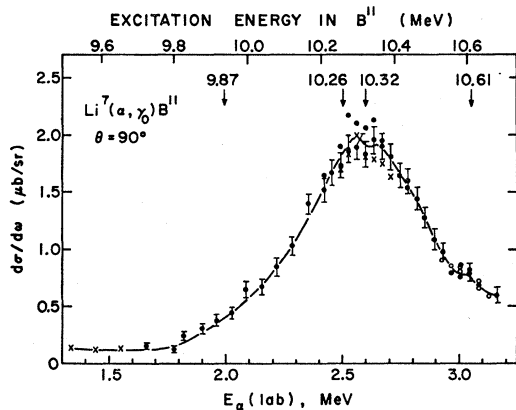


FIG. 5. Excitation function of the capture reaction  $Li^7(\alpha, \gamma_0)B^{11}$ , measured at  $90^\circ$  to beam axis. Arrows indicate position of previously reported states (Ref. 3) in  $B^{11}$ . The cross section calibration is described in the text. Typical errors shown contain statistics and analysis uncertainties. The data points for different target-spot positions are shown by different symbols. The solid line is a smooth curve drawn through the data points.

objective is to obtain a consistent fit (i.e., with the same parameters) to the  $I$  and  $C$  curves, both in absolute scale and energy dependence. The free parameters are resonance energy  $E_0$ ,  $\gamma$  width  $\Gamma\gamma_0$ , the reduced particle widths  $\gamma_{\alpha,l^2}$ ,  $\gamma_{\alpha',l^2}$  for each level, and channel radius  $R$  (assumed to be equal for both channels). Since spins and parities are not known in this region, all possible combinations are considered. This same procedure was applied by Cusson<sup>9</sup> to a simultaneous fit of his elastic ( $E$ ) and inelastic ( $I$ ) curves, using a seven-level formula over a wider range of energies. Listed in Table I are the values which he obtains for the relevant parameters in the region covered by our work. Up to two partial waves are allowed in the incoming channel. In principle, use of these parameters permits direct analysis of  $C$  and extraction of a set of radiative widths for the resonances which are observed. However, the following considerations may suggest caution in the use of Cusson's parameters: First, the agreement achieved for  $E$  is only marginal, at least in the region where  $C$  shows a large cross section. Of course, fits to elastic cross sections over wide resonances are generally bad and are more sensitive to the choice of parameters than  $I$  or  $C$ . Second, Cusson is forced to use two radii;  $R=6$  F for the resonance part and  $R=3.8$  F for the potential scattering background. Six fermis is an unusually large channel radius for this low-mass region. (The  $A^{1/3}$  dependence using  $r_0=1.4$  F yields 4.9 F.) Consequently he obtains some reduced widths exceeding the Wigner limit by factors of 2 and more (see Table I). Cusson offers some arguments in justifying his procedure and it should be noted that similar difficulties with large reduced widths and large radii have been encountered before<sup>4</sup> in the reaction  $Li^7(\alpha, \gamma)$  at resonances below 1 MeV. Thus it is not impossible that the  $(Li^7+\alpha)$  channel has a peculiar radius perhaps indicative of a cluster-type configuration for those states in  $B^{11}$  observed strongly in this channel. Such clustering would also explain the large reduced widths.

The total cross section  $I$  can have interference effects only if two levels of the same spin and parity are overlapping in energy. Neglecting this possibility,  $I$  can be represented as the sum of a sequence of single-level

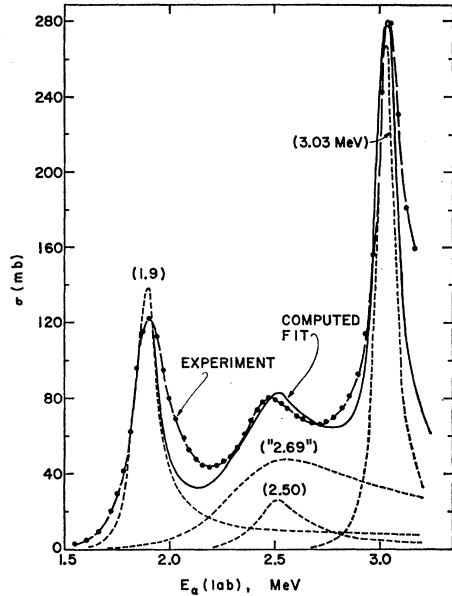


FIG. 6. Fit to the inelastic scattering cross section with the parameters of Table II ( $R=4.9$  F). Three levels at 1.90, 2.48, and 3.04 MeV suffice to explain the excitation function and the absolute cross section.

formulas of the form<sup>17</sup> (adjusted for the present case)

$$\sigma(\alpha, \alpha') = \frac{1}{2} \pi \lambda \alpha^2 (2J+1) \frac{(\sum_l \Gamma_{\alpha l})(\sum_{l'} \Gamma_{\alpha' l'})}{(E_0 + \Delta - E_\alpha)^2 + \Gamma^2/4}, \quad (2)$$

with  $\Gamma_{\alpha l} = 2P_{\alpha l} \gamma_{\alpha l}^2$  and  $\Delta = \sum_{ii} [- (S_{ii} - B_i) \gamma_{ii}^2]$ ,  $\Gamma = \sum_{ii} \Gamma_{ii}$  ( $i=1, 2$ ).  $P_l$  and  $S_l$  are the usual penetration and shift functions.  $B_i$  are suitable boundary conditions which may be conveniently chosen so that  $\Delta=0$  for  $E_\alpha = E_0$ . From Eq. (2) a very useful relation [good to first order in  $(E_\alpha - E_0)$ ] has been derived between the experimentally observed width  $\Gamma_{ob}$  (full width at half-maximum) and the actual width  $\Gamma$ :

$$\Gamma_{ob} = \sum_{ii} \frac{\Gamma}{(1 - d\Delta_i/dE)_{E_0}} = \frac{\Gamma}{1 + \sum_{ii} (dS_{ii}/dE)_{E_0} \gamma_{ii}^2}, \quad (i=1, 2). \quad (3)$$

Using a set of single levels as given by Eq. (2) we calculated a curve for  $I$  using the parameters listed in Table I (for  $R=6$  F). The calculations were performed on the Stanford PDP-7 computer with a program<sup>18</sup> computing Coulomb wave functions and evaluating Eq. (2) for the case of two channels and at most two partial waves in each channel. The computed cross sections are compared with our experimental data in Fig. 6. On the basis of Cusson's spin-parity assignments (assigning a different combination to each level) the

<sup>17</sup> A. M. Lane and R. G. Thomas, Rev. Mod. Phys. **30**, 257 (1958).

<sup>18</sup> P. Paul and N. G. Puttaswamy, Stanford University SCANS Report No. 7a, 1966 (unpublished).

TABLE II. Resonances and parameters obtained from a fit to inelastic scattering for two different interaction radii. Only one partial wave is assumed for each channel.  $\Gamma_{ob}$  is the total resonance width observed in the excitation function.

$E_R$ (lab) (MeV)	$\sigma(\alpha, \alpha')$ (mb)	$\Gamma_{ob}$ (keV)	$J^\pi$	$l$	$l'$	$\gamma_{\alpha^2}$ (MeV)	$\gamma_{\alpha'^2}$ (MeV)	$\gamma_{\pi^2}$ (MeV)	$R$ (F)					
1.9	120	140	$\frac{3}{2}^-$	$s$	$d$	0.394	3.79	0.683	6.0					
			$\frac{3}{2}^+$	$p$	$p$	0.163	0.205							
			$\frac{5}{2}^-$	$d$	$s$	0.916	1.158							
			$\frac{3}{2}^+$	$p$	$p$	0.511	0.810			1.00	4.9			
			$\frac{3}{2}^-$	$s$	$d$	0.121	0.128			0.683	6.0			
			$\frac{1}{2}^+$	$p$	$p$	0.141	0.094			0.05	0.443			
2.48	55	350	$\frac{3}{2}^+$	$p$	$p$	0.155	0.039	0.683	6.0					
			$\frac{5}{2}^+$	$p$	$f$	0.269	0.813							
			$\frac{1}{2}^-$	$d$	$s$	0.346	0.066							
			$\frac{3}{2}^-$	$d$	$d$	0.484	0.181							
			$\frac{5}{2}^-$	$d$	$d$	0.473	0.110							
			$\frac{3}{2}^+$	$f$	$p$	0.229	0.663							
			$\frac{3}{2}^-$	$s$	$d$	0.223	0.460			1.00	4.9			
			$\frac{3}{2}^+$	$p$	$p$	0.306	0.091			0.082	2.283			
			$\frac{1}{2}^+$	$p$	$p$	0.292	0.231			0.152	1.593			
			$\frac{1}{2}^-$	$d$	$s$	1.365	0.184			0.274	0.488			
			3.04	234	70	$\frac{7}{2}^+$	$f$			$f$	0.101	0.163	0.683	6.0
											0.060	0.400		
			$\frac{7}{2}^+$	$f$	$f$	0.640	1.21	1.00	4.9					

single-level approximation should work up to the 3.04-MeV level. The agreement with our data is indeed not bad except in the region of the 1.9-MeV resonance. Cusson's curve gives a peak value of 137 mb while Li and Sherr's<sup>8</sup> experiment gave 110 mb. Our value is 122

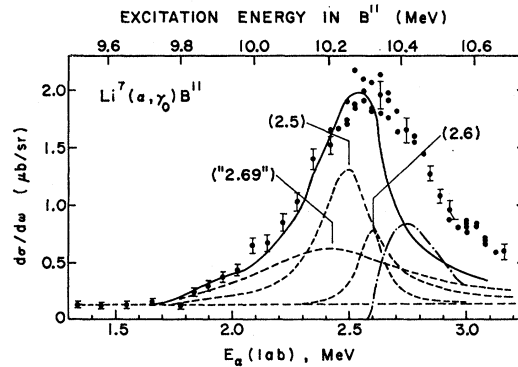


FIG. 7. Fit to the capture cross section using the parameters of Table I ( $R=6.0$  F). Three levels reported by Cusson are labeled by their elastic scattering resonance energies. For each level the radiative width (i.e., the height) is adjusted for best over-all fit. The sum of the three contributions (indicated by the solid line) leaves an excess yield around 2.75 MeV indicated by the dot-dashed line.

TABLE III. Resonance parameters, radiative capture cross section, and radiative widths obtained from a fit to inelastic and capture cross section for  $R=4.9 F$   $\gamma_{W^2}=1.0$  MeV.  $\Gamma$  is total width computed at  $E_R$ .  $\Gamma_{\gamma W}$  are Weisskopf estimates for  $r_0=1.4 F$ .

$E_R$ (lab) (MeV)	$E_{ex}$ in $B^{11}$ (MeV)	$J^\pi$	$\Gamma$ (c.m.) (keV)	$\gamma_{\alpha^2}$ (MeV)	$\gamma_{\alpha'^2}$ (MeV)	$\Gamma_I/\Gamma_E$	$d\sigma/d\Omega$ ( $\mu\text{b}/\text{sr}$ )	$\Gamma_{\gamma 0}$ (eV)	$\Gamma_{\gamma W}$ (eV)
1.90	9.88	$\frac{3}{2}^+$	290	0.511	0.810	0.18	<0.1	<0.5	(E1) 450 <sup>a</sup>
2.48	10.24	$\frac{3}{2}^-$	433	0.227	0.460	0.13	1.5	17	(E1) 500 <sup>a</sup> (M1) 23
2.60	10.32	$\frac{5}{2}^-$	100	0.09 <sup>b</sup>	0.17 <sup>b</sup>	0.00	1.1	1.0	(M1) 25 (E2) 1
2.80	10.45	?	$\sim 140^c$	large	small	<1	$\sim 0.8$	$10/(2J+1)$	
3.04	10.60	$\frac{7}{2}^+$	90	0.640	1.21	0.49	$\leq 0.12$	$\leq 0.2$	(M2) 0.02

<sup>a</sup> An empirical factor of 0.1 is often applied to the E1 Weisskopf estimates.  
<sup>b</sup> These values are taken from Cusson's work (Table I).

<sup>c</sup> Observed width.

mb. Cusson's and our curves have both been normalized to the one of Li and Sherr. Thus the large absolute error in the cross section does not apply.

The capture cross section was then calculated from Eq. (2) (with the proper changes), using the same set of parameters. The absolute peak values are adjusted for each level to obtain the best over-all agreement with the  $C$  curve of Fig. 5. This leads to a set of radiative widths  $\Gamma_{\gamma 0}$ . It should be emphasized that, of course, the  $C$  curve does not actually represent the total capture cross section but the differential cross section at  $90^\circ$ . Therefore, interference effects in the angular distribution between states of identical  $J$  but different parities can in principle alter the resonance shapes from what was obtained in  $I$ . However, at  $\theta=90^\circ$  all odd Legendre polynomials vanish, and thus at this angle such effects are expected to be small.

Figure 7 shows the best fit achieved for  $C$  with the levels obtained by Cusson in the fit of  $I$  and  $E$ . The

resonance suggested by Cusson at 2.69 MeV would induce a peak at 2.4 MeV in  $C$ . A superposition of this resonance and the one at 2.50 MeV gives in fact good agreement with the low-energy side of the experimentally observed structure in  $C$ . On the high-energy side, however, even the inclusion of the narrow level at 2.6 MeV leaves an excess yield centered around 2.80 MeV. Table II lists the radiative capture cross sections and radiative widths which follow from the fit shown in Fig. 7. Obviously the value of 310 eV for the 2.69-MeV level is unreasonably large; however, without this level the experimental yield in  $C$  around 2.3 MeV cannot be explained. It thus appears that Cusson's parameters lead to difficulties when explaining the capture cross section. Actually they give only a very qualitative fit to the elastic-scattering cross section itself in the energy region where a large capture yield is observed.

We therefore followed the second procedure outlined above, which consists of analyzing the  $I$  and  $C$  curves simultaneously to obtain a new set of parameters. No quantitative reference is made to  $E$  but obvious discrepancies are avoided. Analysis begins with the  $I$  curve and the almost totally resolved peak at 1.9 MeV. A preliminary fit to the data by hand gave an observed width  $\Gamma_{ob}$ . With  $\Gamma_{ob}$  and peak cross section  $\sigma$  Eqs. (2) and (3) can be solved exactly for a given  $R$  to obtain the reduced widths  $\gamma_{\alpha^2}$  and  $\gamma_{\alpha'^2}$  (only one  $l$  is considered in each channel). With this starting solution a fit to the peak was computed using Eq. (2) and subtracted from the experimental curve. The procedure was then repeated for the next peak. This analysis gives a fit with the smallest number of levels but is, of course, not unique. The radius was varied between 3.8 and 6.0  $F$  to investigate the need for the large value found by Cusson. The fit achieved for  $R=4.9 F$  ( $r_0=1.4 F$ ) is shown in Fig. 8. Apparently, three resonances at 1.9, 2.48, and 3.04 MeV suffice to explain the inelastic cross section. Table II lists the reduced widths which gave a fit for  $I$  for various spins and parities. Reduction of  $R$  from 6.0 to 4.9  $F$  reduces the number of possible spins and parities considerably. Use of a lower value did not restrict the choice further. Only solutions are listed for which the reduced widths do not exceed the

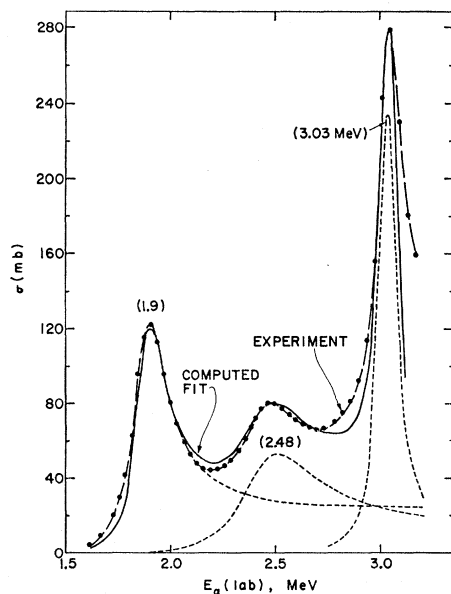


FIG. 8. A fit to the inelastic scattering cross section assuming a sequence of single levels. Level positions and resonance parameters have been taken from Cusson's work (Ref. 9) (see Table I).

Wigner limit by more than a factor of 2. Choosing for each level the spin and parity that was either unique and/or suggested by Cusson, the corresponding reduced widths were used to compute the radiative capture cross section. Figure 9 gives the fit obtained with the radiative widths listed in Table III. The wide level at 2.48 MeV matches the low-energy side of *C* very well and contains most of the yield. The sharp level at 2.6 MeV is not observed in *I* but is very pronounced in *E*. Therefore, we used in this case Cusson's experimental values for the  $\alpha$  width. Again, as in Fig. 7, a strong peak around 2.8 MeV remains unexplained. Attempts to change the 2.6-MeV resonance so as to remove this discrepancy were not successful. One possible explanation is that this peak is in fact responsible for the excess  $\alpha$  yield in *E* which led Cusson to introduce the 2.69-MeV level in his fit. It is also possible that such a level could account for the excess counts in the analysis of *I* (see Fig. 8) around 2.8 MeV. A comparison of Tables I and III shows that both analyses give, in fact, rather similar radiative cross sections for the established resonances. Details will be discussed in the next section.

## 5. RESULTS

### A. 1.9 MeV

Both Cusson's and the present analysis give  $J^\pi = \frac{3}{2}^+$  for this level. For any radius smaller than 6 F this is the only choice. However, while Cusson obtains  $\Gamma_I/\Gamma_E = 4.0$  (see Table I), our analysis of *I* alone yields 0.2 (the complementary solution). The latter ratio leads to a total elastic-scattering cross section of 670 mb. This large value is certainly in contradiction to the elastic-scattering data of Cusson. It was therefore re-investigated under what conditions  $\Gamma_I/\Gamma_E > 1$  could be achieved. The result, entirely in agreement with Cusson's conclusion, was that such a ratio could only be obtained for a radius of 6 F (or larger) and that the cross section and width had to be restricted to values of  $\sigma > 135$  mb and  $\Gamma_{ob} < 110$  keV in order to obtain a reduced width  $\gamma_{\alpha^2}$  or  $\gamma_{\alpha^2} < 3$  MeV (the Wigner limit  $\gamma_W^2 = 0.68$  MeV). For  $R = 4.9$  F, no solution existed for any reasonable magnitudes for  $\sigma$  and  $\Gamma_{ob}$  when  $\Gamma_I/\Gamma_E > 1$ . Since both 135 mb and 100 keV appear to be in disagreement with the data, the situation is, at present, confused (although perhaps not unexpectedly so).

Both Tables I and III show an upper limit of 0.1  $\mu\text{b}/\text{sr}$  for the capture cross section. This limit is based on the possibility that, although the fits of Figs. 7 and 9 do not suggest this, all events at 1.9 MeV could be attributed to this resonance. (Assuming our resonance fits as valid, the actual resonance cross section at 1.9 MeV must be at least five times smaller than the limits in Tables I and III.) The radiative width extracted

from this cross section depends on  $\Gamma_I/\Gamma_E$ . One obtains  $\Gamma_{\gamma 0} \leq 0.5$  eV from Table III and  $\Gamma_{\gamma 0} \leq 1.9$  eV from Table I. The Weisskopf estimate  $\Gamma_{\gamma W}$  for an *E1* transition (for  $r_0 = 1.40$  F) is 450 eV. Typically,  $\Gamma_{\gamma}(E1) \simeq 0.1\Gamma_{\gamma W}(E1)$  in light nuclei.<sup>19</sup> Hence, assuming the expected *E1* multipolarity, the transition from the 9.88-MeV level appears to be very weak.

### B. 2.48 MeV

This resonance corresponds to a state in B<sup>11</sup> at 10.26 MeV. Cusson tentatively assigns  $J^\pi = \frac{3}{2}^-$  and a width of 200 keV. The present analysis gives solutions for  $J^\pi = \frac{1}{2}^\pm, \frac{3}{2}^\pm$  and for a width of 433 keV. Both this width and the ratio  $\Gamma_I/\Gamma_E = 0.13$ , to be compared with 0.04 in Cusson's work, are quite compatible with the elastic-scattering data. The calculated curves in Figs. 6 and 8, obtained as before from the two types of analyses, assume  $J^\pi = \frac{3}{2}^-$ . The excellent and *consistent* agreement with the experimental *I* and *C* curves (Figs. 8 and 9) below 2.5 MeV clearly eliminates any need, at least from this work, for an additional level (such as the broad one with  $\Gamma \simeq 4$  MeV at 2.69 MeV postulated by Cusson) contributing significantly below 2.5 MeV. The radiative capture cross sections due to this transition are 1.5  $\mu\text{b}/\text{sr}$  and 1.2  $\mu\text{b}/\text{sr}$ , respectively. The parameters of Table III yield a radiative width  $\Gamma_{\gamma 0} = 17$  eV; the ones of Table I give  $\Gamma_{\gamma 0} = 5$  eV. Weisskopf estimates are 500 eV for *E1* (or 50 eV, assuming the usual empirical reduction factor) and 23 eV for *M1*. Considering the observed distribution of *E1* and *M1* transition strengths in light nuclei,<sup>19</sup> both radiative widths are easily compatible with either multipole character.

### C. 2.60 MeV

Independent evidence for a level at 10.32 MeV comes from work on the B<sup>10</sup>(*d,p*)B<sup>11</sup> reaction which indicates a level width of  $\Gamma = (54 \pm 17)$  keV.<sup>6</sup> Elastic  $\alpha$  scattering shows a pronounced resonance at this same energy. Cusson extracts from his data a best value of

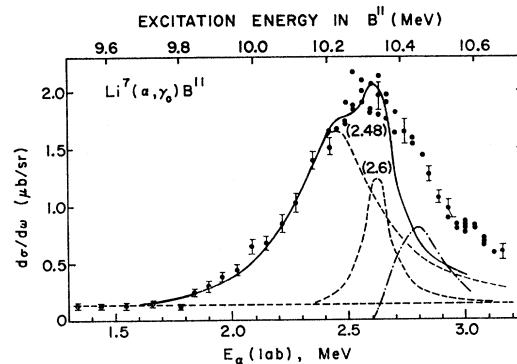


FIG. 9. Fit to the capture cross section using levels and parameters from the fit shown in Fig. 8 ( $R = 4.9$  F). The height of the two known contributing resonances are adjusted for best over-all fit. The sum leaves an excess yield around 2.8 MeV indicated by the dot-dashed line.

<sup>19</sup> E. K. Warburton, *Isobaric Spin in Nuclear Physics* (Academic Press Inc., New York, 1966), p. 90.



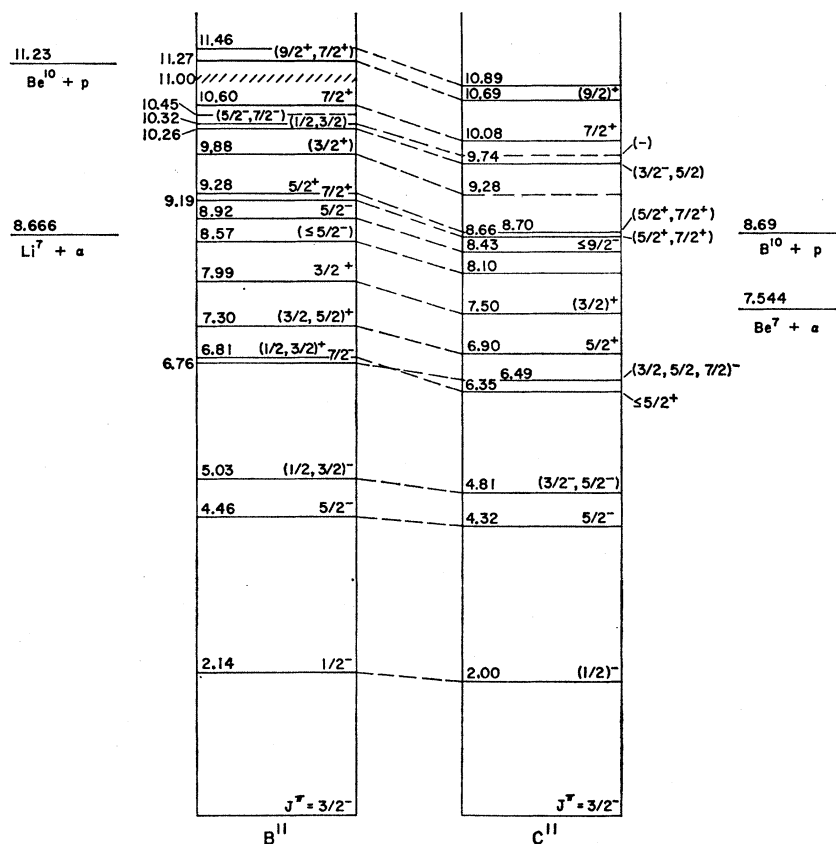


FIG. 10. Comparison of the level schemes of  $B^{11}$  and  $C^{11}$ . Most of this diagram is due to Cusson (Ref. 9). The proposed state in  $B^{11}$  at 10.45 MeV is also shown. The probable analog states are connected by dashed lines.

$\Gamma = 100$  keV and  $J^\pi = \frac{5}{2}^-$  or  $\frac{7}{2}^-$ . The state is not observed in inelastic scattering. We include this level in the capture analysis because of the sharp feature observed at 2.63 MeV. Fits shown in Figs. 7 and 9 lead to the capture cross sections appearing in Tables I and III. A radiative width  $\Gamma_{\gamma 0} \simeq 1$  eV is obtained for both cases using essentially Cusson's parameters with the choice  $J^\pi = \frac{5}{2}^-$ . Weisskopf estimates are 25 eV for an  $M1$  and 1 eV for an  $E2$  transition. Thus both assignments  $J^\pi = \frac{5}{2}^-$  and  $\frac{7}{2}^-$  lead to transition strengths of reasonable magnitude. The possibility was considered that the peak at 2.63 MeV is not due to the level reported in the  $(d, p)$  reaction but rather to another level of larger width which in addition contributes the excess yield at about 2.8 MeV seen in Fig. 9. It was found that the total structure in the capture excitation function could not be explained by two broad peaks alone. The presence of the narrow 2.6-MeV resonance is definitely required.

#### D. 2.80 MeV

The results of both analyses shown in Figs. 7 and 9 indicate an additional peak in the region of 2.80 MeV. This "peak" cannot be attributed to Cusson's assumed state at 2.69 MeV, at least not with the width of 4 MeV obtained in his calculations. However, it is encouraging that a fit for  $E$  leads to the assumption of a new level in this energy region. It appears quite con-

ceivable that a reanalysis of  $E$  would lead to better agreement between the results of our analysis of  $C$  and Cusson's analysis of his elastic data. We therefore tentatively postulate a state at  $10.45 \pm 0.05$  MeV with a c.m. width estimated to be about 140 keV. Since this resonance has at most only a small effect on the  $I$  curve (see Fig. 8), it follows that  $\Gamma_I/\Gamma_B \ll 1$ . If we assume  $\Gamma_a \simeq \Gamma_{ob}$  the capture cross section of about  $0.8 \mu\text{b/sr}$  leads to  $(2J+1)\Gamma_{\gamma 0} = 10$  eV. The differential elastic-scattering cross section is then of the order of 11 mb/sr at  $90^\circ$ , perfectly compatible with the elastic-scattering data.<sup>9</sup>

#### E. 3.04 MeV

This resonance is very prominent in elastic and inelastic scattering. Good fits are obtained to both  $E$  and  $I$ . Cusson<sup>9</sup> assigns  $J^\pi = \frac{7}{2}^+$  to this state. Analysis of  $I$  alone also leads to this assignment. In fact, the parameters obtained from the two different analyses agree well for this peak (compare Tables I and III). A ground-state  $\gamma$  transition from this state thus should have  $M2(E3)$  character. Assuming an  $M2$  transition strength of 1 Weisskopf unit ( $\Gamma_{\gamma W} = 0.015$  eV for  $r_0 = 1.4$  F), one expects a capture cross section of about 5 nb/sr. A larger radius would not increase this value by more than a factor of two. The above estimate of the radiative capture cross section is therefore barely within the range of detectability given the accuracy of  $C$

TABLE IV. Properties of some possible analog states in C<sup>11</sup> obtained from B<sup>10</sup>+p.

$E_p$ (MeV)	$E_{exc}$ (MeV)	Reaction	$J^\pi$	$\Gamma$ (keV)	Partial width (keV)	$\sigma(p,\gamma_0)$ ( $\mu\text{b}$ )	Reference
1.14	9.74	$(p,\alpha_0), (p,\gamma_0)$	$\frac{3}{2}^-$	540	$\Gamma_\alpha=500, \Gamma_{\gamma_0}=0.005, \Gamma_p=40$	3.5	a
1.20	9.74	$(p,\gamma_0)$				7.5	b
1.146	9.74	$(p,\gamma_0)$		414		5.5	c
1.14	9.74	$(p,\gamma_0)$		450			
1.17	9.74	$(p,\alpha_0)$	$\frac{3}{2}(-)$	300	$\Gamma_p=225, \Gamma_{\alpha_0}=75^d$		e
~1.17	9.74	$(p,p)$	$\frac{5}{2}(\pm), (\frac{3}{2}^-)$	300	$\Gamma_p=255, \Gamma_{\alpha_0}=45^d$		f
1.50	10.08	$(p,\alpha_0), (p,\alpha_1)$	$\frac{3}{2}^+$	250	$\Gamma_p=160, \Gamma_{\alpha_1}=34, \Gamma_{\alpha_0}=56$ or $\Gamma_p=90, \Gamma_{\alpha_1}=60, \Gamma_{\alpha_0}=32$		e
1.50	10.08	$(p,p)$	$\frac{5}{2}^+$ or $\frac{7}{2}^+$	250	$\Gamma_{p_0}=90, \Gamma_{\alpha_0}=100, \Gamma_{\alpha_1}=60$		f

<sup>a</sup> Reference 21.

<sup>b</sup> Reference 20.

<sup>c</sup> Reference 22.

<sup>d</sup> Or the complementary set of values.

<sup>e</sup> Reference 23.

<sup>f</sup> Reference 24.

(Fig. 5). In general,  $M2$  transition strengths in light nuclei are less than 1 Weisskopf unit.<sup>19</sup> We do not consider the small bump evident in  $C$  at 3.04 MeV sufficiently outside the statistical error to establish the existence of the transition.

## 6. ANALOG STATES IN C<sup>11</sup>

Some experimental information is available on states in C<sup>11</sup> which may be the analogs of the group of states in B<sup>11</sup> presently under discussion. Figure 10 compares the relevant parts of the two level schemes. Up to the 9.28-MeV state in B<sup>11</sup> Olness *et al.*<sup>1</sup> assign analogs in C<sup>11</sup>, the highest one being the state at 8.70 MeV. Evidence for higher states comes from resonances in the reaction B<sup>10</sup>+p which has a  $Q$  value of 8.7 MeV. Established are resonances at 1.14 MeV in  $(p,\gamma_0)$ ,<sup>20-22</sup> at 1.17 and 1.5 MeV in  $(p,\alpha)$ ,<sup>22,23</sup> and  $(p,p)$ .<sup>24</sup> Table IV lists the properties of these resonances. As noted by Cusson,<sup>9</sup> the 1.5-MeV resonance is certainly the analog of the 10.62-MeV state in B<sup>11</sup> having correct spin and parity and similar partial widths. The proton channel, of course, is closed for this state in B<sup>11</sup> which accounts for the difference in total width.

Assuming that the resonances observed in C<sup>11</sup> at 1.14 and 1.17 MeV are identical, the associated state has a  $\Gamma_{\gamma_0}$  of about 5 eV. Thus it is a likely candidate as the analog of either the 10.26- or the 10.32-MeV state in B<sup>11</sup>. The partial widths listed in Table IV for the 9.74-MeV state agree with the corresponding values of either the 10.26-MeV (2.48 MeV) or 10.32-MeV (2.60-MeV) states (see Tables I and III). On the basis of the somewhat better agreement of the total widths (note that the proton width of the C<sup>11</sup> state is only 50 keV), the value of  $\Gamma_{\gamma_0}$ , and the tentative spin-parity assignment, preference is given to the identification of the 9.74-MeV state in C<sup>11</sup> as the analog of the one at

10.26 MeV in B<sup>11</sup>. Unfortunately though, the situation is not unambiguous. Overley and Whaling<sup>24</sup> observe an anomaly at 1.2 MeV in elastic proton scattering on B<sup>10</sup> which they assign to a  $\frac{5}{2}(\pm)$  level in C<sup>11</sup>. However, they note that the presence of two overlapping levels could resolve the discrepancy existing between the  $(p,\alpha_0)$  and the  $(p,p)$  data. Existence of two levels in this energy region would parallel the situation in B<sup>11</sup>. However, the available B<sup>10 $(p,\gamma_0)$ C<sup>11</sup> data show little indication of any other resonance except the one at 1.74 MeV, although some variance existed between data taken at 0°<sup>22</sup> and 90°.<sup>20</sup> We have remeasured the excitation function of the reaction B<sup>10</sup> $(p,\gamma_0)$ C<sup>11</sup> at 90° up to a bombarding energy of 1.7 MeV, i.e., beyond the 10.08-MeV state. The resulting curve, shown in Fig. 11, is completely consistent with previous data<sup>22</sup> at 0° since it indicates a single broad resonance [ $\Gamma(\text{c.m.})=450$  keV] at 1.14 MeV. The symmetry of the resonance curve would seem to exclude the presence of any other strong resonance in this energy region. Tentatively, we therefore relate the 10.26-MeV state in B<sup>11</sup> to the 9.74-MeV state in C<sup>11</sup>. The 10.32-MeV level is observed strongly</sup>

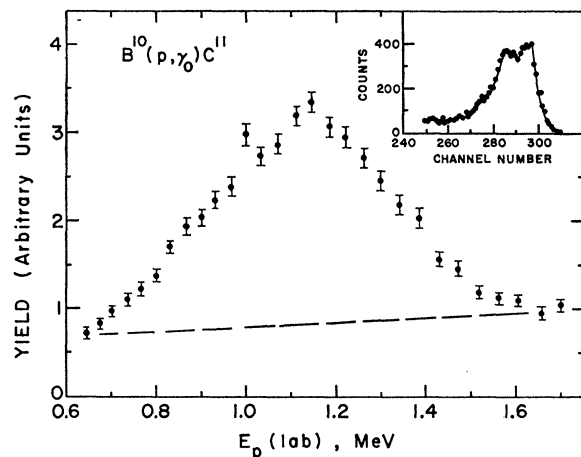


FIG. 11. Excitation function of the B<sup>10</sup> $(p,\gamma_0)$ C<sup>11</sup> reaction at 90° to the beam axis. The insert shows the ground-state transition obtained with the  $\gamma$ -detection system described in the text.

<sup>20</sup> R. B. Day and T. Huus, Phys. Rev. **95**, 1003 (1954).

<sup>21</sup> G. B. Chadwick, T. K. Alexander, and J. B. Warren, Can. J. Phys. **34**, 381 (1956).

<sup>22</sup> S. E. Hunt, R. A. Poppe, and W. W. Evans, Phys. Rev. **106**, 1012 (1957).

<sup>23</sup> J. W. Cronin, Phys. Rev. **101**, 298 (1956).

<sup>24</sup> J. C. Overley and W. Whaling, Phys. Rev. **128**, 315 (1962).

TABLE V. States and ground-state transition strengths predicted in  $B^{11}$  by the general two-body matrix element calculations of Kurath.<sup>a</sup>  $\Lambda_0$  is the square of the transition matrix element. The values listed for  $\Gamma_{\gamma_0}$  have been computed assuming probable values for the spin  $I_1$  of the resonant state.

$E_{exc}$ (MeV)	$J^\pi$	$(2I_1+1)\Lambda_0(M1)$	$\Gamma_{\gamma_0}$ (eV)
10.69	$\frac{3}{2}^-$	0.10	0.06
11.44	$\frac{3}{2}^-$	0.14	0.15
11.62	$\frac{1}{2}^-$	0.50	1.09
12.02	$\frac{3}{2}^-$	0.17	0.41
12.65	$\frac{7}{2}^-$		

<sup>a</sup> Reference 27.

in the  $B^{11}(d,p)$  reaction. The analog state in  $C^{11}$  might therefore have such a large proton width that the  $\gamma$  transition (proportional to  $\Gamma_\gamma/\Gamma_p$ ) is not observed within the present level of sensitivity.

## 7. DISCUSSION

Recent data on inelastic electron scattering on  $B^{11}$  may be compared to the  $\gamma$  widths presented here. Kossanyi-Demay and Vanpraet<sup>25</sup> report a broad peak around an excitation energy of 9 MeV which they analyze in terms of states at 7.9, 8.92, and 9.5 MeV. The peak cannot be due to the well-known states at 9.19 or 9.28 MeV since the quoted strength exceeds the well-known ground-state  $\gamma$  widths for these states<sup>4,5</sup> by several orders of magnitude. It is suggested that the observed peak is instead related to either the 10.26- or 10.32-MeV states. The value of 5 eV for an  $M1$  transition strength quoted from the scattering data is in fair (Table II) to good (Table I) agreement with our results for the 10.26-MeV state.

Theoretical calculations for odd-parity states in  $B^{11}$  have been published recently by two groups.<sup>2,26</sup> Their results differ mainly above the  $\frac{7}{2}^-$  state at 6.76 MeV. Amit and Katz<sup>26</sup> make spin-parity assignments for several higher states in disagreement with presently available experimental evidence.<sup>1</sup> The calculation by Cohen and Kurath<sup>2</sup> has been compared to experiment by Olness *et al.*<sup>1</sup> The agreement with level assignments and  $\gamma$ -decay branching ratios up to the 8.92-MeV state is good. The energies and  $M1$  ground-state transition strengths for the next five levels obtained by Kurath<sup>27</sup> are listed in Table V. It is apparent that, despite occur-

rence of two levels with  $J^\pi = \frac{3}{2}^-$  and  $\frac{5}{2}^-$  in the approximate energy region, the theoretical values for  $\Gamma_{\gamma_0}$  are much smaller than the experimental values listed in Tables I and III for the 10.26- or 10.32-MeV levels. For the  $\frac{3}{2}^-$  level theory also predicts a strong transition to the first excited state which is not observed.

Considering the fact that the levels presently discussed are well bound with respect to both single-particle channels, the disagreement between experiment and the shell-model predictions is somewhat disturbing. It may attest to the fact that the states observed in  $\alpha$  capture are of a special nature as is also suggested by the large radii which emerged from the  $R$ -matrix analysis.

A qualitative model taking into account the possible special structure describes the states in terms of  $(Li^7 + \alpha)$  clusters. It certainly can explain the large  $\alpha$ -particle reduced widths. It does not, however, lead to better agreement with the  $\gamma$  width as we now briefly discuss: For instance, assume the spin assignments  $\frac{3}{2}$  and  $\frac{5}{2}$  with negative parity for the states of 10.26 and 10.32 MeV, respectively. The simplest such state would consist of  $s$ - and  $d$ -wave  $\alpha$  particles about a  $Li^7$  core containing the ground and first excited state in the ratio of the respective reduced  $\alpha$  widths (see Tables I and III). The  $B^{11}$  ground state would have to contain rather substantial amounts of these same configurations to generate  $M1$  ground-state transitions as large as the observed values. One would expect the first excited state to be similar in nature and the absence of a  $M1$  transition from the 10.26-MeV state is again unexplained.

Positive-parity states with  $J = \frac{3}{2}$  or  $\frac{5}{2}$  like the state at 9.88 MeV (neither can this parity be excluded at present for the 10.26- and 10.32-MeV states) would be formed by a  $p$ -wave  $\alpha$  particle around the  $Li^7$  core. Although in this case the transitions  $10.26 \rightarrow 0$  and  $10.32 \rightarrow 0$  could be accounted for with a much smaller cluster admixture into the ground state, neither the absence of the first-excited-state transition(s) nor the small  $\gamma$  width of the 9.88-MeV state can be readily understood without the introduction of some special circumstance, e.g., cancellation of matrix elements.

## ACKNOWLEDGMENTS

We are indebted to Professor S. S. Hanna for helpful discussions, to Professor S. L. Blatt for his help in the early stages of the experiment, and to Dr. D. Kurath for supplying the shell-model wave functions.

<sup>25</sup> P. Kossanyi-Demay and G. J. Vanpraet, Nucl. Phys. **81**, 529 (1966).

<sup>26</sup> D. Amit and A. Katz, Nucl. Phys. **58**, 388 (1964).

<sup>27</sup> D. Kurath (private communication).